Non-Oscillation Physics at a Neutrino Factory

INTRODUCTION

Aside from neutrino oscillation physics, a neutrino factory will also be a formidable tool for other physics such as deep inelastic scattering experiments and searches for exotic neutrino interactions. The neutrino factory parameters considered in this study represent improvements of 3-4 **orders of magnitude** over existing neutrino beams. Table **??** compares the numbers of neutrinos produced by present beamlines. Besides the high intensity, a muon storage ring neutrino source has two other important aspects not found in current neutrino beams. First, since the kinematics of muon decay are well understood and because of the degree of control we will have over the muons in the storage ring, the neutrino flux will be known to a much higher accuracy than in any other high energy neutrino beam. Second, the neutrino factory will not only be a source of high energy muon neutrinos, but also electron neutrinos as well. The rest of this section is a short introduction to the phenomenology of deep inelastic scattering followed descriptions of possible experimental measurents. Later sections are devoted to searches for novel effects which may appear in neutrino beams with 10^4 time the intensity of present beams.

table equivalent to Kevin's comparing NuTeV, MINOS, CERN, Nufac

Possible subsection on statistics.....table and/or figures from Heidi...

STRUCTURE FUNCTION MEASUREMENTS

In considering measurements of structure functions in neutrino interactions it is important to remember that almost all present-day experiments have relied on heavy (isoscalar) targets with an approximately equal mix of protons and anti-protons. Such measurements have essentially been the average of neutron and proton structure functions with additional unknown A dependent effects. In addition, most measurements have been of the average of neutrino and anti-neutrino structure functions. We have only really measured one fourth of the possible combinations of $\nu/\overline{\nu}$ neutron/proton. In addition, no measurements of the spin dependent structure functions have been made in neutrino scattering. At a neutrino factory, we can expect to perform measurements with excellent statistics and good flux estimates on polarized and unpolarized hydrogen and deuterium targets. With these data, we should be able to determine the real structure functions instead of averages.

Statistics

Overview of statistics

Kinematics

In neutrino scattering, the incoming beam can assumed to be massless ($m_\nu \simeq 0$) but the outgoing lepton mass may be important. If E'_{lab} denotes the laboratory frame energy of the scattered lepton ℓ,

$$\mathbf{q} = \mathbf{k}_\nu - \mathbf{k}_\ell, \qquad Q^2 = -\mathbf{q}^2 = 2E_\ell E_\nu - m_\ell^2 - 2E_\nu p_\ell \cos\theta_{lab} \tag{1}$$
$$\nu = (\mathbf{p}_\mathrm{q}\mathbf{q})/ME_\mathrm{lab} - E'_\mathrm{lab} \tag{2}$$
$$x = Q^2/2M\nu \tag{3}$$
$$y = M\nu/(\mathbf{k}_\nu \mathbf{p}_\mathrm{q}) = (1 + cos\theta_{CM})/2 \approx \nu/E_\mathrm{lab} \tag{4}$$
$$W^2 = m_4^2 c^4 = 2M\nu + M^2 - Q^2 \tag{5}$$

where, M is the target nucleon mass, E_ν is the incoming neutrino energy E_ℓ, p_ℓ are the outgoing lepton energy and momentum θ_{lab} is the lepton angle with respect to the incoming beam. $\mathbf{q}$ is the four-momentum transfer to the target, ν is the energy transfer, x is the Bjorken x variable, y is the scaled energy transfer and W^2 is the invariant mass of the final state hadronic system squared.

Neutrino Scattering

Un-polarized

For an unpolarized target the neutrino(anti-neutrino) scattering cross section is:

$$\frac{d\sigma^{\nu(\overline{\nu})}}{dxdy} = \frac{M_W^4 G_F^2 M E_\nu}{\pi(Q^2 + M_W^2)^2}\Big[y^2 x F_1(x,Q^2) + (1 - y - \frac{M^2 xy}{s - M^2})F_2(x,Q^2) \pm (y - \frac{y^2}{2})xF_3(x,Q^2)\Big] \tag{6}$$

where M is the mass of the target and the F_i are Structure Functions. $2xF_1$ is purely transverse while $F_2 = 2xF_1 + F_L$ where F_L is a purely longitudinal structure function. F_3 enters with a '-' sign for anti-neutrino scattering.

In the limit that $Q << E, M_W$, this can be rewritten as:

$$\frac{d\sigma^{\nu(\overline{\nu})}}{dxdy} = \frac{M_W^4 G_F^2 M E_\nu}{2\pi(Q^2)^2}[F_2(x,Q^2)[1 + (1-y)^2] \pm xF_3(x,Q^2)[1 - (1-y)^2] + (1-y)F_L(x,Q^2) \tag{7}$$

Polarized Scattering

If the target is longitudinally polarized with respect to the neutrino polarization, then the cross section difference:

$$\frac{d^2(\sigma_{\Rightarrow}^{\leftarrow} - \sigma_{\Leftarrow}^{\leftarrow})^{\nu(\bar{\nu})}}{dxdy} = \frac{M_W^4 G_F^2 M E_\nu}{\pi(Q^2 + M_W^2)^2}\{\pm y(1 - \frac{y}{2} - \frac{xyM}{2E})xg_1 \mp \frac{x^2 yM}{E}g_2 + y^2 x(1 + \frac{xM}{E})g_3 + (1 - y - \frac{xyM}{2E})[(1 + \frac{xM}{E})g_4 + g_5]\}, \tag{8}$$

is described by two parity conserving Polarized Structure Functions g_1 and g_2, and by three parity violating Polarized Structure Functions g_3, g_4 and g_5. However, if the nucleon is transversely polarized:

$$\frac{d^2(\sigma_{\Uparrow}^{\leftarrow}-\sigma_{\Downarrow}^{\leftarrow})^{\nu(\bar\nu)}}{dxdy} = \frac{M_W^4G_F^2M}{16\pi^2(M_W^2+Q^2)^2}\sqrt{xyM\left[2(1-y)E-xyM\right]}\{\mp 2xy(\frac{y}{2}g_1+g_2) \quad (9)$$
$$+xy^2g_3+(1-y-\frac{xyM}{2E})g_4-\frac{y}{2}g_5\}.$$

The transverse cross section is suppressed by M/Q with respect to the longitudinal cross section.

Quark Parton Model

Because discussions of the quark-parton model for neutrino interactions often include assumptions which are reasonable for isoscalar targets but not for the general case, it is worth going through the parton model predictions and their relation to structure functions.

In the quark parton model quarks have probability $\mathrm{q}_i(x)$ of carrying momentum fraction x of the proton momentum. The function $\mathrm{q}_i(x)$ is called a parton distribution function or PDF. Typical PDF's are shown in Figure **??**.

For the kinematic regime being considered at present neutrino factories, we can restrict ourselves to the lightest 4 quark species, (ud), (cs). Generalization to b is reasonably simple.

If one integrates over the final state and (for the moment) ignores the masses of the quarks, the scattering cross section is that for two point fermions and has the simple form.

$$\frac{d\sigma^\nu}{dxdy} = \frac{4M_W^4G_F^2ME_\nu x}{\pi(Q^2+M_W^2)^2}\left[\left[\mathrm{d}_L(x)+\mathrm{s}_L(x)\right]+\left[\overline{\mathrm{u}}_R(x)+\overline{\mathrm{c}}_R(x)\right](1-y)^2\right] \quad (10)$$

Here we have explicitly put in the probability for a quark to have the correct helicity. For an unpolarized target $\mathrm{q}_L(x)=\mathrm{q}_R(x)=\frac{1}{2}\mathrm{q}(x)$. For a polarized quark $\mathrm{q}_L(x)=\frac{1}{2}(\mathrm{q}(x)+\Delta\mathrm{q}(x))$ and $\mathrm{q}_R(x)=\frac{1}{2}(\mathrm{q}(x)-\Delta\mathrm{q}(x))$ where $\Delta\mathrm{q}(x)$ is the degree to which the quark spin is aligned with the proton spin. $(1-y)$ is a helicity factor from the scattering from the right-handed anti-quarks.

For anti-neutrinos

$$\frac{d\sigma^{\overline{\nu}}}{dxdy} = \frac{4M_W^4G_F^2ME_\nu x}{\pi(Q^2+M_W^2)^2}\left[\left[\overline{\mathrm{d}}_R(x)+\overline{\mathrm{s}}_R(x)\right]+\left[\mathrm{u}_L(x)+\mathrm{c}_L(x)\right](1-y)^2\right] \quad (11)$$

Parton Model predictions for structure functions

For unpolarized targets this implies the following parton model interpretation for the structure functions:

$$2xF_1^{\nu p}(x,Q^2) \simeq F_2^{\nu p}(x,Q^2) = 2x[\overline{\mathrm{u}}(x)+\mathrm{d}(x)+\overline{\mathrm{c}}(x)+\mathrm{s}(x)] \quad (12)$$
$$2xF_1^{\overline{\nu}p}(x,Q^2) \simeq F_2^{\overline{n}up}(x,Q^2) = 2x[\mathrm{u}(x)+\overline{\mathrm{d}}(x)+\mathrm{c}(x)+\overline{\mathrm{s}}(x)] \quad (13)$$
$$xF_3^{\nu p}(x,Q^2) = 2x[\mathrm{d}(x)-\overline{\mathrm{u}}(x)+\mathrm{s}(x)-\overline{\mathrm{c}}(x)] \quad (14)$$
$$xF_3^{\overline{\nu}p}(x,Q^2) = 2x[\mathrm{u}(x)-\overline{\mathrm{d}}(x)+\mathrm{c}(x)-\overline{\mathrm{s}}(x)] \quad (15)$$

For polarized targets:

$$g_1^{\nu p}(x,Q^2) = \delta \mathrm{d}(x,Q^2) + \delta \mathrm{s}(x,Q^2) + \delta \overline{\mathrm{u}}(x,Q^2) + \delta \overline{\mathrm{c}}(x,Q^2), \tag{16}$$
$$g_1^{\bar{\nu} p}(x,Q^2) = \delta u(x,Q^2) + \delta c(x,Q^2) + \delta \overline{\mathrm{d}}(x,Q^2) + \delta \overline{\mathrm{s}}(x,Q^2), \tag{17}$$

where $\delta q = q^{\uparrow\uparrow} - q^{\uparrow\downarrow}$ is the difference between the parton densities of quarks polarized parallel or antiparallel to the nucleon spin, and $\Delta q = \delta q + \delta \overline{\mathrm{q}}$ is the net helicity of the quark along the nucleon spin. g_2 has a 'Wandzura-Wilczek' like relation. That is it consist of a twist–2 (g_2^{WW}) and a twist–3 ($\bar{g}_2$) contribution and it has a difficult partonic interpretation,

$$g_2 = g_2^{WW} + \bar{g}_2; \qquad g_2^{WW}(x,Q^2) = -g_1(x,Q^2) + \int_x^1 \frac{dy}{y} g_1(y,Q^2) \tag{18}$$

For g_3 and $g_4 + g_5$ one can get the parton model expressions:

$$(2x)^{-1} g_{4+5}^{\nu p}(x,Q^2) = g_3^{\nu p}(x,Q^2) = -[\delta d(x,Q^2) + \delta s(x,Q^2) - \delta \overline{\mathrm{u}}(x,Q^2) - \delta \overline{\mathrm{c}}(x,Q^2)], \tag{19}$$
$$(2x)^{-1} g_{4+5}^{\bar{\nu} p}(x,Q^2) = g_3^{\bar{\nu} p}(x,Q^2) = -[\delta u(x,Q^2) + \delta c(x,Q^2) - \delta \overline{\mathrm{d}}(x,Q^2) - \delta \overline{\mathrm{s}}(x,Q^2)], \tag{20}$$

Scattering from neutrons

If one assumes that isospin predicts that $\mathrm{u}_n = \mathrm{d}_p$ and similar equations for the rest of the quarks, then the cross sections for scattering from neutrons can be rewritten in terms of the proton parton distributions as: For W exchange on neutrons:

If we assume that $\mathrm{s}(x) = \overline{\mathrm{s}}(x)$ and $\mathrm{c}(x) = \overline{\mathrm{c}}$ then the structure functions for charged current neutrino scattering from an iso-scalar target can be related to the parton distributions inside the proton:

$$F_2 = x \sum_i \Big[\mathrm{q}_i(x) + \overline{\mathrm{q}}_i(x)\Big] \tag{21}$$

$$xF_3 = x \sum_i \Big[\mathrm{q}_i(x) - \overline{\mathrm{q}}_i(x) \pm 2x[\mathrm{s}(x) - \mathrm{c}(x)]\Big] \tag{22}$$

These are the structure functions generally quoted in the neutrino literature.

Neutrino data and charged lepton scattering on deuterium can be related via:

$$2xF_1^{\gamma d}(x,Q^2) \simeq F_2^{\gamma d}(x,Q^2) = x \sum_i q_i^2 [\mathrm{q}_i(x) + \overline{\mathrm{q}}_i(x)] \approx \frac{5}{18} F_2^{\nu N}(x,Q^2) \tag{23}$$

Neutral Current Scattering

Neutral current scattering proceeds via the exchange of a Z_0 boson and is not believed to include flavor changing processes.

The neutral current processes can be written as:

$$\frac{d\sigma_N^{\nu p}C}{dxdy} = \frac{2M_W^4 G_F^2 M E_\nu}{\pi(Q^2+M_W^2)^2} x\Big[[L_{\mathrm{d}}^2 + R_{\mathrm{d}}^2(1-y)^2](\mathrm{d}(x)+\mathrm{s}(x)] + [L_{\mathrm{u}}^2(1-y)^2 + R_{\mathrm{u}}^2][\overline{\mathrm{u}}(x)+\overline{\mathrm{c}}(x)]\Big] \quad (24)$$

$$\frac{d\sigma_N^{\overline{\nu} p}C}{dxdy} = \frac{2M_W^4 G_F^2 M E_\nu}{\pi(Q^2+M_W^2)^2} x\Big[[L_{\mathrm{u}}^2(1-y)^2 + R_{\mathrm{u}}^2](\mathrm{u}(x)+\mathrm{c}(x)] + [L_{\mathrm{d}}^2 + R_{\mathrm{d}}^2(1-y)^2][\overline{\mathrm{d}}(x)+\overline{\mathrm{s}}(x)]\Big] \quad (25)$$

(This is from Conrad Shaevitz and Bolton, need to check as doesn't use separate quark/anti-quark couplings)

Where the L_q and R_q are the left and right handed weak couplings for quarks of type 'd' or 'u'.

Table 1 summarizes these couplings:

$$\begin{array}{lll} & L_q & R_q \\ \mathrm{u,c} & +\frac{1}{2}-\frac{2}{3}\sin^2\theta_W & -\dfrac{2}{3}\sin^2\theta_W \\ \mathrm{d,s} & -\frac{1}{2}+\frac{1}{3}\sin^2\theta_W & +\dfrac{1}{3}\sin^2\theta_W \end{array} \quad \begin{array}{r}(26)\\(27)\\(28)\\(29)\end{array}$$

The couplings for left-handed anti-quarks are the same as those for right-handed quarks and vice versa.

STUDYING NUCLEAR QCD WITH NEUTRINOS

Introduction

In addition to reminding the high-energy community that there is a rich field of non-oscillation physics that should be an integral part of the muon collider/storage-ring concept, it is also important to reach out to other physics communities who could join us in support of a neutrino factory facility through a non-oscillation physics program. Among the more obvious facilities to approach is the nuclear community. This community has seldom had the opportunity to do nuclear physics with neutrinos due to the low intensity of past neutrino beams and the consequent need for the heaviest practical target (Fe) to accumulate large statistics. The NuMI/MINOS beam could offer a first systematic look at nuclear QCD with a range of higher A targets, but it will not be until a neutrino factory from a muon storage ring or collider that a nuclear program, including important H_2 and D_2 target normalizations, can be undertaken.

Although there are topics that are purely nuclear such as the form factor study described by Gerry Garvey in these proceedings, there is a class of experiments which bridges the nuclear and high energy community. This is the analysis of nuclear effects in the extraction of structure functions. These nuclear effects have been studied extensively using muon and electron beams but have only been glanced at in low-statistics bubble chamber experiments using neutrinos. If we consider the behavior of the ratio R_A of $F_2(x,Q^2)$ measured on a nucleus (A) to $F_2(x,Q^2)$ measured on a nucleon as a function of x_{Bj} we pass through four distinct regions in going from $x_{Bj}=0$ to $x_{Bj}=1.0$:

1. "shadowing" up to $x_{Bj}=0.1$,
2. "anti-shadowing for $0.1 < x_{Bj} < 0.2$,
3. the "EMC Effect" for $0.2 < x_{Bj} < 0.7$ and
4. "Fermi motion effects" for $x_{Bj} > 0.7$.

Outline of a Muon Storage Ring Neutrino Nuclear Effects Experiment

As we discuss possible physics topics we will refer to an experiment which assumes a 50 GeV storage ring with a detector 50 m away from an 800 m straight section. With 10^{20} mu decays per year per straight section, we would expect 4 x 10^6 ν_{mu} and 1.7 x 10^6 $\overline{\nu_e}$ interactions per kg-year in a fiducial volume of radius 10 cm. The detector would consist of a liquid D_2 target followed by a rotating support of different A targets - similar to the geometry of the Fermilab E-665 Tevatron muon experiment. To acquire 10^7 events per year in all targets we would need targets with fiducial volume r = 10 cm and length of 50 cm for D_2 3.7 cm for C and 0.45 cm for W. The liquid H_2 or D_2 targets could be CCD coupled active liquid targets (ie Bubble Chambers!) which could provide tracking within the target, followed by the higher A targets interspersed with tracking chambers, followed by appropriate calorimetry and muon identification/measurement techniques.

The challenge for the experiment is finding tracking and calorimetry which can accurately measure the hadron energy without being flooded with neutrino interactions themselves.

Shadowing Region

As mentioned these effects have been studied with electromagnetic probes and a pertinent question is to ask what additional things can we learn when using a weak probe. In the shadowing region there are several effects that should yield a different ratio R_A when using neutrinos as the probe. In the limit $Q^2 --> 0$, the vector current is conserved and goes to 0, however the axial-vector part of the weak current is only partially conserved (PCAC) and $F_2(x, Q^2) -->$ a non-zero constant as $Q^2 --> 0$. According to the Adler theorem [1] the cross section of ν_μ - N can be related to the cross section for π - N at $Q^2 = 0$. What effect does a nuclear environment have on the Adler theorem?

As we increase Q^2 from 0 but keep it under 10 GeV^2 in the shadowing region we enter the region of vector meson dominance (VMD) in μ/e - A scattering. The physics concept of VMD is the dissociation of the virtual photon into a q - $\overline{q}$ pair one of which interacts strongly with the "surface" nucleons of the target nucleus (thus the "surface" nucleons "shadow" interior nucleons). In ν - A scattering there is an additional contribution from axial-vector mesons that is not present in μ/e - A scattering. Boros et al [2] predict that the resulting shadowing effects in ν - A scattering will be roughly 1/2 that measured in μ/e - A scattering.

In a more quantitative analysis, Kulagin [3] used a non-perturbative parton model to predict shadowing effects in ν - A scattering. At 5 GeV^2 he predicts equal or slightly more shadowing in ν - A scattering than in μ/e - A scattering. He also attempts to determine quark flavor dependence of shadowing effects by separately predicting the shadowing observed in $F_2(x, Q^2)$ (sum of all quarks) and $xF_3(x, Q^2)$ (valance quarks only). Fig. 1 shows the results of a 2 year run using predictions of Kulagin's model for F_2 and xF_3. The proposed comparison of W:D_2 would exhibit a much sharper decrease in the ratio as x_{Bj} decreases. As can be seen, the predicted difference between the shadowing on sea and valence quarks is clearly visible down to x_{Bj} = 0.02 - 0.03.

FIGURES

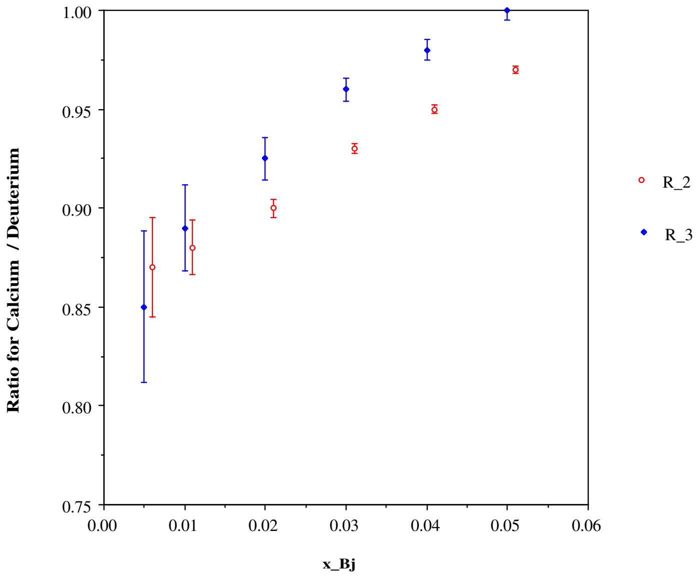

FIG. 1. $R_{Ca:D_2}$ for both F_2 and xF_3 as measured in a 2 year exposure at the facility described in the text.

Anti-shadowing Region

Drell-Yan experiments have also measured nuclear effects. Their results are quite similar to DIS experiments in the shadowing region. However, in the anti-shadowing region where R_A makes a brief but statistically significant excursion above 1.0 in DIS, Drell-Yan experiments see no effect. This could be an indication of difference in nuclear effects between valence and sea quarks. Eskola et al [4] quantified this difference by using a leading order/leading twist DGLAP model which used initial nuclear parton distributions from CTEQ4L and GRV-LO and assumed scale evolution of nuclear parton distribution is perturbative. The model predicts that the difference between nuclear effects in $xF_3(x,Q^2)$ and $F_2(x,Q^2)$ persist through the anti-shadowing region as well. Taking the work of Kulagin and Eskola together implies that nuclear effects in $xF_3(x,Q^2)$ should be quite dramatic with more shadowing than $F_2(x,Q^2)$ at lower x and then R_A rising fairly rapidly to yield significant antishadowing around $x = 0.1$. In our standard 2 year experiment we should be able to measure antishadowing effects and the difference between shadowing effects in $F_2(x,Q^2)$ and $xF_3(x,Q^2)$ to the 6 σ statistical level

EMC-effect Region

To determine individual quark contributions to the EMC-effect will be challenging since the participation of sea quarks, and thus the difference between $F_2(x, Q^2)$ and $xF_3(x, Q^2)$, shrinks rapidly with increasing x_{Bj}. However, Eskola's predictions for this region indicate that the contribution of $\overline{u}$ and $\overline{d}$ to R_A in the Q^2 range of this experiment remains well below 1 so that the quantity $R(2)_A$ - $R(3)_A$ should remain negative well into the EMC-effect region.

Behavior of $F_2(x, Q^2)$ as $x_{Bj} --> 1$ in a Nuclear Environment

When working in the "fermi-motion" region it has been shown that we need to add more than the Fermi gas model to a simple nucleon to reproduce the behavior of $F_2(x, Q^2)$ at high x_{Bj}. Few-nucleon-correlation models and multi-quark cluster models allow quarks to have a higher momentum which translates into a high-x_{Bj} tail. In this region $F_2(x, Q^2)$ should behave as $e^{-ax_{Bj}}$. There have been analysis of this behavior in similar kinematic domains using μ + C and ν + Fe interactions. The muon experiment finds a = 16.5 +- 0.5 while the neutrino experiment finds a = 8.3 +- 0.7 +- 0.7 (systematic). Is the value of a dependent on the nucleus? One would expect any few nucleon correlation or multi-quark effects to have already saturated by Carbon. Is a dependent on the probe?

Summary

There is a very rich program of studying nuclear effects with a neutrino probe in a high statistics neutrino factory experiment. The effects could be measured to statistically significant accuracy in a 2 year exposure to the beam in the near-detector experiment described above. The data gathered would allow separate measurements of the effects on valence quarks and sea quarks across much of the x_{Bj} range.

The nuclear community should be informed of what a valuable tool for nuclear research awaits them in the neutrino factory facility.

PRECISION ELECTROWEAK MEASUREMENTS AT A NEUTRINO FACTORY

Introduction

Precision measurements of electroweak parameters from neutrino experiments have played an important role in testing the Standard Model and in probing new physics. However, previous neutrino deep inelstic scttering (DIS) experiments have been limited by a lack of statistics and by the coarse granularity of their detectors.

The intense flux of neutrinos from a neutrino factory opens up a whole new era of precision electroweak measurements that were previously limited by statistics.

A precision measurement of $\sin^2\theta_W$or M_W could very well still be important 10 years from now. At that time the best measurement of $M_W(\pm 30\text{MeV})$ would have come from Fermilab Tevatron collider experiments and LEP-II, and the LHC experiments will be vigorously looking for the Higgs, if it had not already been found. Therefore, complementary mesurements of electroweak parameters from an independent experiment could play crucial role in LHC experiments' advancements. In this section, we discuss the prospects of a precision measurement of $\sin^2\theta_W$and the mass of the W boson (M_W) at a neutrino factory facility.

Previous Measurements

It is always a good idea to learn from past experiments to better understand what can be done in a future facility. The CCFR neutrino experiment extracted $\sin^2\theta_W$ [5,6] through a measurement of the ratio of the NC to CC cross sections, as expressed in the following Llewellyn-Smith formula [7] :

$$R^{\nu(\overline{\nu})} = \frac{\sigma_{NC}^{\nu(\overline{\nu})}}{\sigma_{CC}^{\nu(\overline{\nu})}} = \rho^2 \left(\frac{1}{2} - \sin^2\theta_W + \frac{5}{9}\sin^4\theta_W \left(1 + \frac{\sigma_{CC}^{\overline{\nu}(\nu)}}{\sigma_{CC}^{\nu(\overline{\nu})}} \right) \right), \tag{30}$$

where the value of ρ depends on the nature of the Higgs sector and has the value $\rho = 1$ in the SM. This method, although it removed much of the uncertainty due to QCD effects in the target, does leave some rather large uncertainties associated with heavy quark production from the quark sea of the nucleon target.

The successor experiment, NuTeV (FNAL-E815) experiment, has improved upon this measurement by using separate neutrino and anti-neutrino beams [8]. Separation of neutrino and anti-neutrino neutral current events allows the utilization of the Paschos-Wolfenstein relationship [9]:

$$r = \frac{\sigma(\overline{\nu}, CC)}{\sigma(\nu, CC)} \simeq 0.5. \tag{31}$$

NuTeV has presented a preliminary result [10] of

$$\sin^2\theta_W = 0.2253 \pm 0.0019(\text{stat}) \pm 0.0010(\text{syst}). \tag{32}$$

There were two dominant systematic uncertainties in the CCFR experiment: 1) ν_e flux and 2) CC charm production. These two major systematic uncertainties in CCFR were been dramatically reduced in the NuTeV experiment, by utilizing sign selected neutrino beam, so that the remaining dominant uncertainty was the statistical uncertainty.

Since neutrinos interact weakly, the past neutrino fixed target experiments have used dense material as neutrino targets in order to increase the interaction rate. The calorimetric nature of the targets does not allow one to distinguish electron neutrino induced charged current interactions (CC) from neutral current (NC) interactions. Thus, these old-style heavy target experimental set-ups (such as NuTev or CCFR) will be fatal for neutrino factory analyses because there always will be both ν_μ $(\overline{\nu}_\mu)$ and $\overline{\nu}_e$ (ν_e) in the beam. This condition necessitates the need for light target detector which is sufficiently different than the normal detectors for neutrino oscillation measurements.

Experimental Technique

As in previous neutrino experiments, the measured quantity used to determine $\sin^2\theta_W$ at a neutrino factory will be the ratio of NC to CC DIS events. However, the NuTeV-style measurement is not accessible at the neutrino factory beam because $\nu_e(\overline{\nu}_e)$ and $\overline{\nu}_\mu(\nu_\mu)$ come in pairs simultaneously and so NC events from neutrinos and those from anti-neutrinos are not distinguishable on an event-by-event basis. This condition restricts the numerator of the ratios to be sum of NC events. In addition, it is necessary to minimize uncertainties in sea quark induced CC production of charm. Large portion of this uncertainty can be canceled out by taking a difference between the neutrino and antineutrino induced CC events. Therefore the two accessible ratios that satisfy both the above conditions are the hybrids of the Llewellyn-Smith ratio in Eq. 30 and Paschos-Wolfenstein parameter in Eq. **??**, as follows:

$$R_\nu^{\mu^-} = \frac{\sigma(\nu_\mu, NC) + \sigma(\overline{\nu}_e, NC)}{\sigma(\nu_\mu, CC) - \sigma(\overline{\nu}_e, CC)} = \frac{R^{\nu_\mu} + grR^{\overline{\nu}_\mu}}{1 - gr} \tag{33}$$

for the $(\nu_\mu\overline{\nu}_e)$ beam, and

$$R_{\overline{\nu}}^{\mu^+} = \frac{\sigma(\overline{\nu}_\mu, NC) + \sigma(\nu_e, NC)}{\sigma(\nu_e, CC) - \sigma(\overline{\nu}_\mu, CC)} = \frac{R^{\nu_\mu} + g^{-1}rR^{\overline{\nu}_\mu}}{1 - g^{-1}r} \tag{34}$$

for the $(\overline{\nu}_\mu\nu_e)$ beam. The expression of $R_\nu^{\mu^-}$ and $R_{\overline{\nu}}^{\mu^+}$ in terms of r, R^{ν_μ} and $R^{\overline{\nu}_\mu}$ assumes lepton universality. The second of the two equations differs from the first only in the replacement of g by g^{-1}, where g is the energy-weighted flux ratio between ν_μ and $\overline{\nu}_e$ or, equivalently, between $\overline{\nu}_\mu$ and ν_e:

$$g \equiv \frac{\int \Phi(E_{\overline{\nu}_e})E_{\overline{\nu}_e}dE_{\overline{\nu}_e}}{\int \Phi(E_{\nu_\mu})E_{\nu_\mu}dE_{\nu_\mu}} = \frac{\int \Phi(E_{\nu_e})E_{\nu_e}dE_{\nu_e}}{\int \Phi(E_{\overline{\nu}_\mu})E_{\overline{\nu}_\mu}dE_{\overline{\nu}_\mu}}. \tag{35}$$

Experimental and Theoretical Issues

While the prospects in greatly improving $\sin^2\theta_W$ measurements in a neutrino factory are good, there are both experimental and theoretical concerns that we need to consider in order to achieve meaningful precision ($\delta\sin^2\theta_W \sim 10^{-3}$).

Experimental Issues

Regarding the beam, a crucial requirement is the ability to reverse the polarity of the ring so that one can choose between $(\nu_\mu\overline{\nu}_e)$ or $(\overline{\nu}_\mu\nu_e)$ beams at any given time. This capability provides the opportunity for studying possible systematics due to the beam of a given flavor.

Probably the most demanding requirement on the detector for this analysis is the ability to distinguish events with primary electrons or muons from neutrino CC interactions from the purely hadronic showers produced in NC interactions. Traditional heavy target neutrino detectors can not distinguish ν_e induced CC interactions from NC interactions. Other particularly relevant capabilities are the use of a light isoscalar target, with a trigger capability, that can provide the charm and strange sea measurements from the same experiment, as this will be very useful in reducing the remaining systematic uncertainties.

In order to satisfy the above requirements, the detector needs to have:

- Good EM and hadronic shower identification.
- High electron detection efficiency along with high efficiency particle identification.
- Good charged particle momentum measurement.
- Good EM and hadronic shower energy containment and measurement.
- Muon identification and momentum measurement.

High-performance low density target detectors for neutrino factory experiments will greatly suppress the expeimental uncertainties in the $\sin^2\theta_W$ measurement relative to today's analyses conducted using coarse-granularity calorimetric neutrino target. Probably the most important remaining experimental systematic in this measurement will be the e/μ identification efficiency. Since the expected and meaningful total error in this measurement is on the order of 10^{-3}, it is extremely vital to control the overall efficiency of the particle identification system to better than 2×10^{-4}. Otherwise every ν_e CC event where the electron escapes identification would be a direct background to NC interactions for both ν_μ and ν_e.

Theoretical Issues

Theoretical uncertainties will be expected to dominate the $\sin^2\theta_W$ measurement at a neutrino factory, and an improved understanding of several potential theoretical uncertainties will be required for a meaningful interpretation of a sub-30 MeV equivalent W mass error.

The CC-charm cross section error needs to be minimized. In principle, this error can be reduced by measuring the CC production cross section of charm directly from the same experiment using vertex-tagged charm events.

Further effects which require investigation include: a) nucleon isospin-violating effects [19]; b) strange quark mass effects in $\nu_\ell \bar{u} \to \ell^- \bar{s}$ and $\nu_\ell s \to \nu_\ell s$; c) Effects from "radiative higher twist processes" such as $\nu_\ell n \to \gamma \ell^- p$; d) other higher twist effects, which are assessed as one of the dominant errors in today's measurements (however, a recent study [14] indicates that most the higher twist effects might be higher order QCD corrections in GLS measurements)

Prospects in $\sin^2\theta_W$ Measurement

Using the neutrino factory beam parameter discussed in Section **??** for mean muon energy of 50GeV and scaling the muon decay rate to 40 m long straight section, one expects approximately 1.5×10^7 ν_μ events per year per 0.5 m long CCD target with a radius of 10 cm. In addition, with a detector that can distinguish electrons and muons resulting from CC interactions and assuming a 100% fiducial acceptance for events occuring in the CCD target, the effective neutrino interaction statistics double, resulting in a total of 3×10^7 events per year. Since the number of neutrino events from the NuTeV experiment (with 3×10^{18} protons-on-target) was on the order of 1 million events for ν_μ, the expected 3×10^7 events per year from the neutrino factory would cause a reduction in the statistical uncertainty by a factor of about five within a year of data taking. This enormous increase in statistical power also helps to minimize many of the systematic uncertainties dramatically. The remaining error of 0.0004 in NuTeV, due to ν_e flux, no longer exists for a detector that is capable of distinguishing CC interactions of ν_e from hadronic showers resulting from NC interactions by identifying the outgoing electrons. The uncertainties resulting from energy scale are also irrelevant because they are associated with the muon range through the muon length cut, which will not be relevant for neutrino factory analysis. The errors in event length, in principle, also no longer contribute, because with the detector described in the following section, one can distinguish CC from NC interactions on an event-by-event basis. The above expectations will enable the experiment to reduce the statistical and experimental systematic uncertainties on $\sin^2\theta_W$ to the equivalent M_W uncertainty of ~ 30 MeV.

Conclusions

This work has demonstrated that precision test of the electroweak Standard Model can be expected to play an important part in the physics program of a neutrino experiment at a neutrino factory. The $\sin^2\theta_W$measurement at the neutrino factory facility, using the the variables in Eq. 33 and Eq. 34 will allow tests of unparalleled statistical accuracy and control over a potentially large theoretical uncertainty in CC production of charm. However, controlling particle ID uncertainty from experimental systematics and understadning higher twist and radiative correction theoretical systematics play crucial role in obtaining meaningful measurements.

HEAVY LEPTON MIXING

A muon storage ring offers ample opportunities to search for new phenomena in yet unexplored physical regions. One such opportunity is the ability to search for the existence of neutral heavy leptons. Several models describe heavy isosinglets that interact and decay by mixing with their lighter neutrino counterparts [20,26]. The high intensity neutrino beam created by the muon storage ring provides an ideal setting to search for neutral heavy leptons with a mass below the muon mass, 105.6 MeV/c^2.

It is postulated that neutral heavy leptons (L_0) could be produced from muon decay when one of the neutrinos mixes with its heavy, isosinglet partner. Neutral heavy leptons can be produced via one of two channels:

$$\mu^- \rightarrow L_0 + \overline{\nu}_e + e^- \tag{36}$$

$$\mu^- \rightarrow \nu_\mu + L_0 + e^- \tag{37}$$

The branching ratio for each of these reactions is given by:

$$BR(\mu \rightarrow L_0 \mu e) = |U_i|^2 (1 - 8x_m^2 + 8x_m^6 - x_m^8 + 12x_m^4 \ln x_m^2) \tag{38}$$

Here $x_m \equiv m_{L_0}/m_\mu$ and $|U_i|^2$ is the mixing constant between the specific type of neutrino and the neutral heavy lepton: $U_i \equiv \langle L_0 | \nu_i \rangle$. Note that $|U_\mu|^2$ and $|U_e|^2$ need not be identical.

Once produced, a neutral heavy lepton of such low mass will either decay via $L_0 \rightarrow \nu\nu\nu$, $L_0 \rightarrow \nu e e$, or $L_0 \rightarrow \gamma\nu$. The most viable mode for detection is the two-electron channel. For this particular decay mode, the L_0 can decay either via charged current or charged and neutral current interactions. The branching ratio for this decay process has been previously calculated [22]. Since the decay width is proportional to U_j^2, the number of L_0's detectable is proportional to $U_i^2 * U_j^2$ in the limit where the distance from the source to the detector is short compared to the lifetime of the L_0.

Using the above model, one can estimate the number of neutral heavy leptons produced at the muon storage ring which later decay within a given detector. The number of detected neutral heavy leptons is given by the equation below:

$$N_{L_0} = N_\nu * BR(\mu \rightarrow L_0 \nu e) * \epsilon * e^{-L/\gamma c \tau} * BR(L_0 \rightarrow detectable) * (1 - e^{-\delta l/\gamma c \tau}) \tag{39}$$

Here N_ν is the number of neutrinos produced from muon decay, $BR(\mu \rightarrow L_0 \nu e)$ is the branching ratio of muons decaying into neutral heavy leptons versus ordinary muon decay, L is the distance from the beamline to the detector, δl is the length of the detector, ϵ is the combined detector and geometric efficiency, τ is the L_0 lifetime, and $BR(L_0 \rightarrow detectable)$ is the branching ratio for the neutral heavy lepton decaying via a detectable channel (presumably $L_0 \rightarrow \nu e e$).

In testing the sensitivity to L_0 production at the muon storage ring, we make a few underlying assumptions. We assume that the storage ring utilizes a pure, unpolarized muon beam with straight sections such that 25 percent of the muons will decay to neutrinos pointing towards the detector. We assume that the fiducial volume is 3 meters in diameter and 30 meters in length, and that the detector has sufficient tracking resolution to detect the e^+e^- vertex from the L_0 decay. We assume for now that the background is negligible. These parameters correspond to the fiducial volume of the decay channel used for the L_0 search at E815 (NuTeV) [23,24].

The sensitivity of the detector has been calculated for a number of different muon energies and beam intensities. Figure 2 shows limits on the L_0-ν_μ mixing as a function of L_0 mass. One achieves the best limits from using relatively low energy/high intensity muon beams. This is a major improvement over previous neutral heavy lepton searches, where limits do not reach below $6.0 * 10^{-6}$ in the low mass region [25,26].

The single event sensitivity quoted here depends greatly on having minimal background levels in the signal region. Part of this can be achieved by kinematic cuts which discriminate against neutrino interactions in the detector material. However, it will probably be necessary to reduce the amount of material in the fiducial region greatly compared to NuTeV. We estimate that even if the decay region is composed only of helium gas, the number of neutrino interactions will approach a few thousand. The ideal detector, therefore, would consist of a long vacuum or quasi-vacuum pipe with appropriate segmentation for tracking. The decay pipe could be used in conjunction with larger neutrino detectors adapted for the muon storage ring.

The muon storage ring may prove to be an ideal location to continue the search for neutral heavy leptons. The high intensity neutrino beam allows for a neutral heavy lepton search to be sensitive to the $10 - 100$ MeV$/c^2$ mass range. In addition, such a neutral heavy lepton program could easily interface with a neutrino detector which uses the same neutrino beam. It is also clear, however, that a neutral heavy lepton search would receive the most benefit at lower muon energies, and thus would yield best results at the earlier stages of the muon storage ring program.

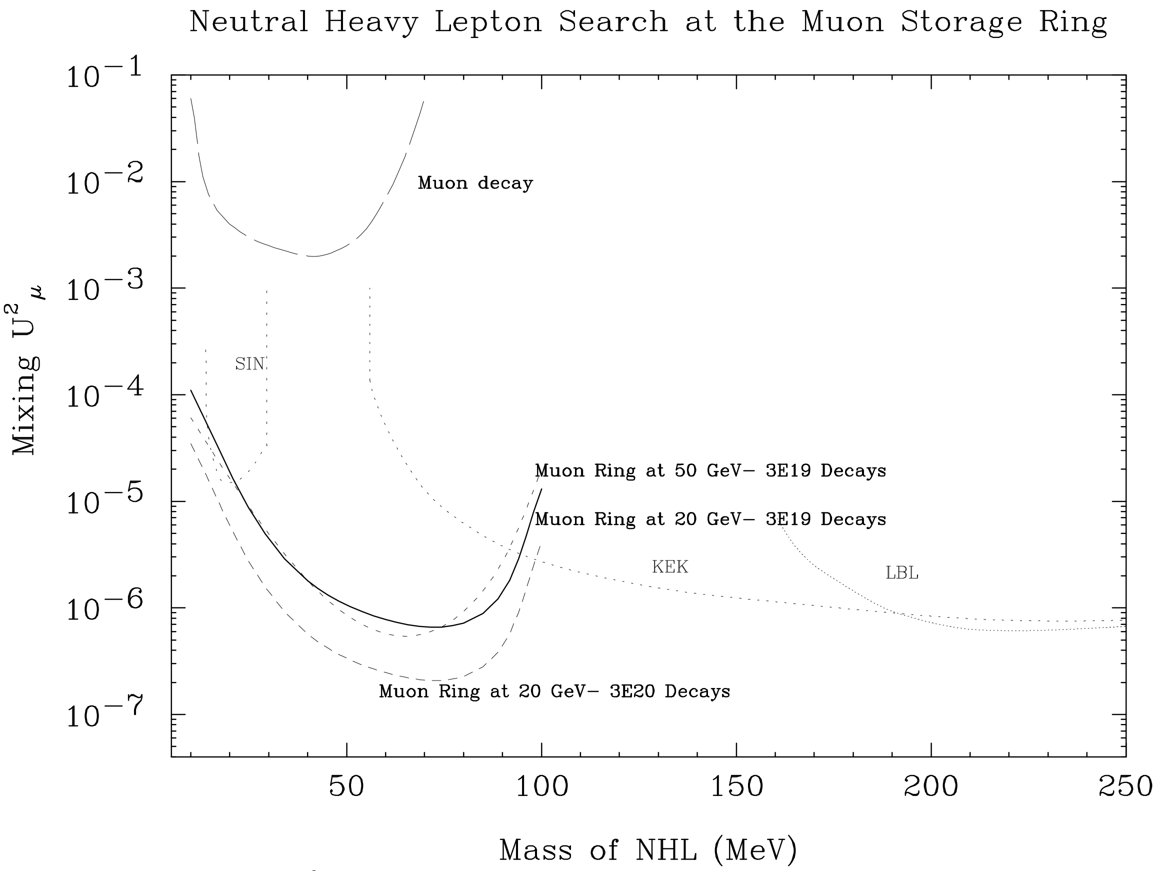

FIG. 2. Limits on $|U_{\mu L}|^2$ as a function of L_0 mass for one year of running. The curves show sensitivities for 20 GeV and 50 GeV muon energies. Sensitivities assume no background events in signal region.

NEUTRINO MAGNETIC MOMENTS

Although neutrino oscillation searches are the primary focus of the neutrino factory study, these searches are sensitive to the mass differences between neutrino eigenstates and not to the absolute scale of the neutrino masses. If discovered, the magnitude of the neutrino magnetic moment (NMM) can provide the actual neutrino eigenstate mass through a direct relationship (Equation 40). A measurement of the NMM would have great importance for the development of stellar models, and knowledge of the neutrino mass would have even greater impact in the field of cosmology. Even failing the goal of a measurement, an improved limit could constrain several Standard Model extensions. As shall be seen, a NMM search can run parasitically as the front–end to a typical long baseline detector.

The following subsections present the current predictions for the magnitude of the NMM, the state of NMM searches today, and the results of a sensitivity study for a novel phase rotation scheme that may improve existing laboratory limits by several orders of magnitude. The final figure provides the means to estimate the statistical power of the result for many different neutrino factory scenarios.

Current Predictions and Limits

Despite their lack of charge, a neutrino can possess a non-zero magnetic moment that can arise through loop diagrams such as Figure ??. In the Standard Model, extended only insofar as the presence of a right–handed neutrino, or such that left–handed neutrinos are allowed to have mass, the expected [27] neutrino magnetic moment magnitude is given by

$$\mu_\nu \simeq 3 \times 10^{-19}\ \mu_{Bohr} \cdot \left(\frac{m_\nu}{1\ \mathrm{eV}}\right), \tag{40}$$

where μ_{Bohr} is the Bohr magneton. Several extensions to the SM would result in a much larger NMM; supersymmeteric models can produce $10^{-14}\mu_{Bohr}$ to $10^{-12}\mu_{Bohr}$ [28] and calculations that invoke large extra dimensions easily yield $10^{-11}\mu_{Bohr}$ or larger [29].

Relative to the SM expectation, the excluded values of NMM are not at all stringent, being seven to nine orders of magnitude larger. The current limits on neutrino magnetic moment from laboratory experiments are $\mu_\nu \leq 1.5$ to $1.8 \times 10^{-10}\mu_{Bohr}$ for electron neutrinos [30] [31] and $\mu_\nu \leq 7.4 \times 10^{-10}\mu_{Bohr}$ for muon neutrinos [32]. Astrophysical limits are stronger: the slow rate of plasmon decay in horizontal branch stars [33] implies $\mu_\nu \lesssim 10^{-11}\mu_{Bohr}$, while the neutrino energy loss rate from supernova 1987a [34] yields $\mu_\nu \lesssim 10^{-12}\mu_{Bohr}$. Note, however, that several assumptions are implicit to the astrophysics limits, including the core temperature of the stars; if stellar models omit important processes, these limits may be overestimated. Also, the supernova limit applies only to Dirac neutrinos and not to the Majorana case.

From the weakness of the current limits, one can infer the difficulty of NMM experiments. Because it would provide a highly–collimated and remarkably intense neutrino beam, the neutrino factory promises to improve the reach of traditional searches as well as to provide a unique opportunity to explore unconventional NMM search methods. The next section describes a suggested search method that could provide this improved reach.

The Phase Rotation Scheme

Existing search schemes possess a weakness that sharply limits their ultimate sensitivity: the formulae for the hypothesized effect are quadratic in μ_ν. In contrast, the following scheme is linear in terms of μ_ν and most other parameters, hence it has a good chance of exceeding the limits from current experiments and possibly the limits from astrophysics calculations. The experiment relies on the principle that a neutrino's helicity state (and therefore its magnetic moment) can be reexpressed in terms of an orthogonal basis. Because the two new components behave differently when exposed to a magnetic field they will no longer sum to the original state. The result is a phase rotation from left–handed helicity to right–handed helicity.

Consider a neutrino of energy E in the presence of a magnetic field B, the particle's energy gains a new term μ_ν·B. Defining the B field along x, with a neutrino travelling (and having helicity) along the z-direction, the helicity and magnetic moment of the neutrino may be decomposed into $+x$ and $-x$ components, yielding a non-zero dot product for the magnetic potential energy for each state:

$$|\uparrow\rangle = \frac{e^{-iEt}}{\sqrt{2}}\,|\leftarrow\rangle + \frac{e^{+iEt}}{\sqrt{2}}\,|\rightarrow\rangle \text{ becomes } \frac{e^{-i(E+V)t}}{\sqrt{2}}\,|\leftarrow\rangle + \frac{e^{+i(E-V)t}}{\sqrt{2}}\,|\rightarrow\rangle\,. \tag{41}$$

Because the magnetic potential has opposite sign for the two energy states, the two states can be split within the magnetic field. The splitting of the $+x$ and $-x$ component states is equivalent to a phase rotation of the neutrino helicity from $|\uparrow\rangle$ toward $|\downarrow\rangle$, i.e. the neutrino can "rotate" to a sterile state in the case of a Dirac neutrino or to an antineutrino in the Majorana case. At a far detector, the signal would be a deficit in the number of neutrinos detected with the B field in place compared the number detected without the B field.

If there is a force on the neutrino, then the magnetic potential energy comes from the B field itself and the energy states are indeed split. If there is no force on the neutrino, then there is no energy exchange with the external field and the magnetic potential energy comes from other contributions to the neutrino energy such that the total neutrino energy remains unchanged. Because the magnetic force on a dipole takes the form $F = \nabla(\mu_\nu\cdot\mathrm{B})$, the presence or absence of a gradient in the B field will determine whether the total energy changes.

In this phase rotation scheme, the neutrino is allowed to see a gradient in the magnetic field which causes the energy states to split. Before the neutrino leaves the influence of the field, the magnetic field energy must be brought to zero homogeneously in space, such that there is no gradient, no magnetic force, and the energy is therefore not returned to the field. The energy difference between the two states then persists indefinitely as do the resulting phase rotations. Ideally, the magnetic field would be placed near the neutrino source for a long baseline experiment; that way, the phase difference between energy states has time to grow and the neutrino will rotate further toward its alternate state.

The Magnetic Field

There are two basic requirements for the magnetic field:

1) The magnetic field must oscillate one quarter cycle while the neutrinos are within the homogeneous part of the field. If the field covers too small an area for a given oscillation frequency, the neutrino will pass through two spatial gradients and the energy states will not remain split. (Because timing is crucial, this study assumes bunched muons in the ring providing bunched neutrinos with negligible longitudinal spread.)

2) The magnetic field must be as strong as possible while still satisfying (1). A strong B-field will maximize the resulting phase rotation angle that occurs in the distance between the cavity and the far detector.

We have explored the possibility [35] of using two existing technologies for the B field, resonant cavities and kicker magnets. In both cases the maximum magnetic field is too small to yield improved magnetic moment limits given realistic equipment.

As an alternative, we envision many superconducting wires comprising a large current sheet, not unlike one wall of existing (~ 2 T) collider detector solenoids. Consider a neutrino passing through an infinite current sheet from left to right. While the neutrino is on the left, the current ramps up from zero to maximum, resulting in a B field that is homogeneous in all space. As the neutrino passes through the sheet, it experiences a magnetic gradient of 2·B. As the neutrino continues to the right, the current drops again to zero, bringing B to zero also. For an actual device, the sheet must be large in comparison to the width of the neutrino beam and also in comparison to the distance travelled by the neutrino in one half cycle of the current.

Superconducting current sheets can provide much larger magnetic fields than any other method explored to date. In addition, given shielding walls placed at appropriate distances, several sheets in series linearly increase the rate of phase rotation.

Sensitivity

The maximum parameter space is explored with the magnetic field(s) in place for approximately 50% of the data collection period. Assuming a small effect, this will maximize the statistical power of the live and null data sets and result in the best chance of resolving any differences that might result. Worth noting: the long baseline detector and intervening material remains the same for both data sets, so most systematic uncertainties cancel exactly in a ratio.

Assuming for simplicity the absence of neutrino oscillations except those that arise from the current sheets, the formula for the number of events lost to sterile states may be expressed very simply as:

$$N_{lost} = N * \sin\left(\mu_\nu \mathrm{B} t\right) \tag{42}$$

Figure 4 compares this result to the expected statistical fluctuations in the CC event rate at a far detector. The y–axis is the significance, simply defined as $N_{lost}/\sqrt{N}$. The x–axis displays the total number of neutrino decays required. The lines assume 5000 CC events expected in the long baseline detector per 10^{19} muon decays [36]. The diagonal lines represent contours of constant "C", where $C = \mu_\nu \mathrm{B}t$ with the given units. For instance, with magnetic gradients totaling 1 Tesla, long baseline distance of 3000 km, and the entry–level neutrino factory (10^{19} muon decays), a NMM of magnitude $10^{-11}\mu_{Bohr}$ would only appear at the one–sigma level of significance.

Because the diagonal lines turn out to be logarithmically–spaced, this formulation allows quick estimation of sensitivity for different parameter scenarios. Consider the example again but with magnetic gradients totalling 3 Tesla; this change essentially results in a new line with $C = 3.16$ and a 3–sigma limit. As can be seen from the figure, the expected sensitivity may be improved by a rough factor of ten for every: factor of ten in magnetic field strength, factor of ten in number of current sheets, factor of ten in distance to the detector, and factor of 100 in muon decays.

Summary

This section has compared the current best neutrino magnetic moment limits to what might be accomplished at a neutrino factory. This study has identified a novel neutrino magnetic moment search technique that is both feasible and has the potential to provide higher sensitivity than prior methods. The method relies on the interaction of the neutrino magnetic moment and an oscillating magnetic field to rotate the neutrino helicity. The strength of the proposed apparatus is that it could run completely transparently as the front–end to a long baseline neutrino oscillation detector. Although the SM prediction for the neutrino magnetic moment lies out of reach even for this type of experiment, such a search at a neutrino factory could constrain several Standard Model extensions that predict larger values for the magnetic moment.

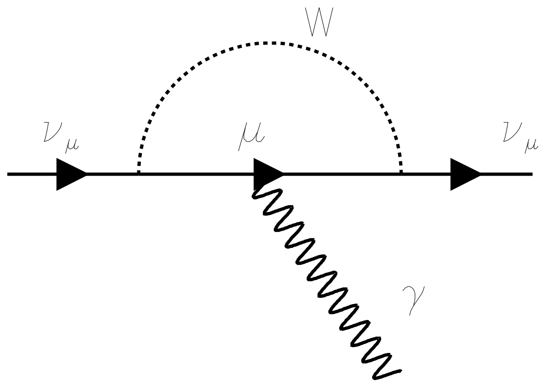

FIG. 3. One possible loop diagram that results in a non–zero neutrino magnetic moment.

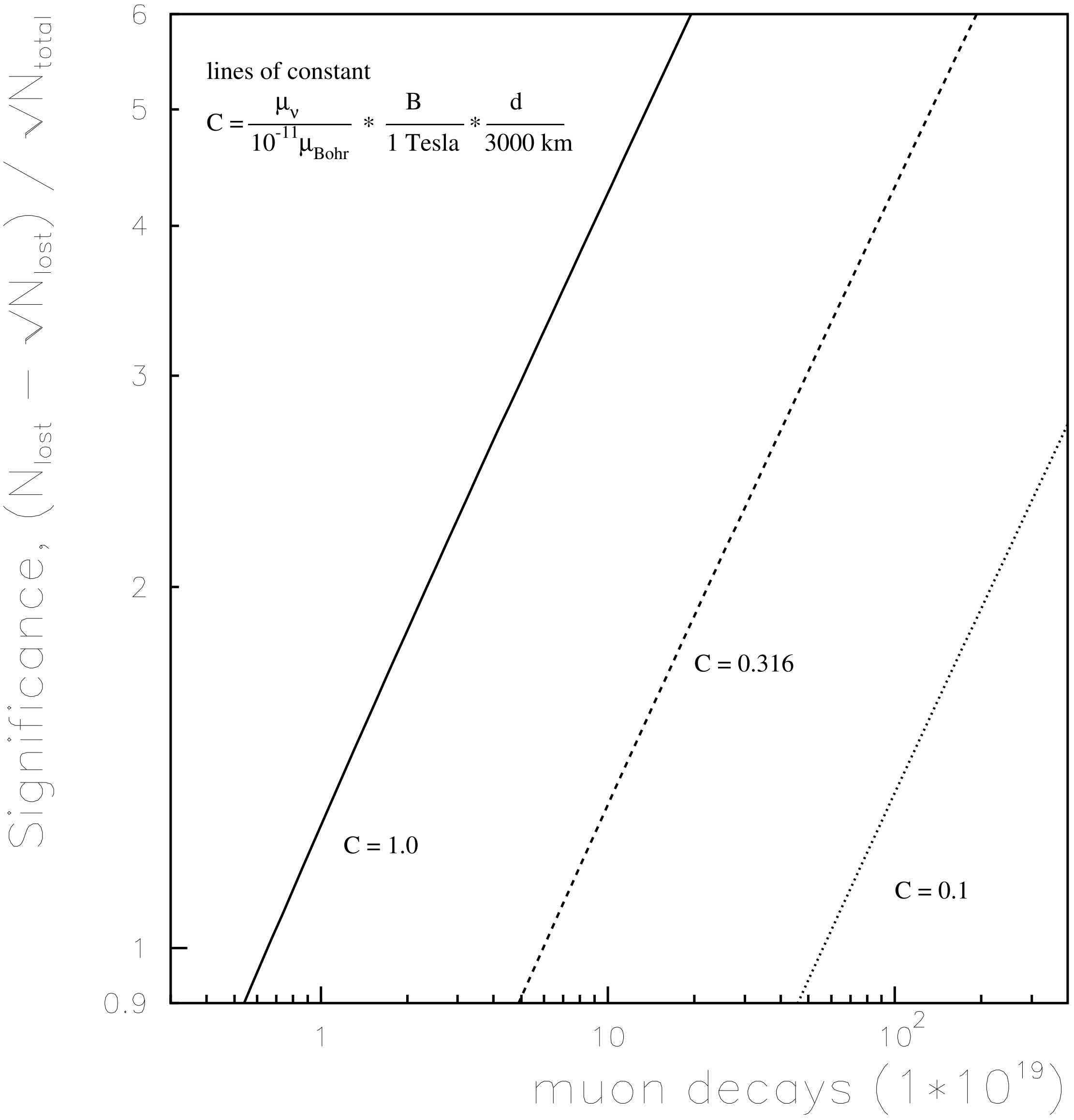

FIG. 4. Significance for several scenarios.

ANOMOLOUS LEPTON PRODUCTION

The neutrino beam from a muon storage ring would consist of a virtually pure combination of $\bar{\nu}_e$ and ν_μ (or charge-conjugate). Also, at the source of the neutrino beam, the $\bar{\nu}_e$ and ν_μ will not have had time to oscillate into other flavors: For a 20 GeV muon storage ring with a 700 m straight section, and neutrino oscillations with $\Delta m^2 = 3.5 \times 10^{-3}$ eV^2, the oscillation probability is $\approx 5 \times 10^{-9}$. Furthermore, the neutrino flux is highest at the source. Thus, an experiment at the neutrino source could be highly sensitive to exotic processes resulting in production of e^-, μ^+, or τ of either charge. While such a search is interesting in its own right, it is also useful to rule out exotic contributions to long-baseline neutrino oscillation signals.

These exotic processes would probably have a flat or rising dependence on the neutrino energy E_ν. In contrast, a neutrino oscillation would have a $1/E_\nu^2$ dependence. Also, if the distance L of the experiment changes, the rate of exotic events would decrease with the flux as $1/L^2$. In contrast, the neutrino oscillation probability would increase as L^2 (for L small compared to the oscillation period), and so the rate of oscillated events would be independent of L. Thus, one could distinguish between exotic processes and the beginning of a neutrino oscillation.

Anomalous lepton production could occur if muons decay to neutrino flavors other than those in the usual decay $\mu \to e\bar{\nu}_e\nu_\mu$, and the anomalous neutrinos then interact in the target. Alternatively, they could be produced if a $\bar{\nu}_e$ or ν_μ interacts with the target via an exotic process.

The only direct experimental limit on exotic $\mu \to e\bar{\nu}_x\nu_y$ decays is $BR(\mu \to e\bar{\nu}_\mu\nu_e) < 1.3\%$ [37]. Indirect limits are also very weak. The contribution of non- $V-A$ interactions to the muon decay rate has been limited to 8% [37]. Also, the total muon decay rate is one of the main measurements used to constrain electroweak parameters [37]. To first order,

$$\frac{1}{\tau_\mu} = \frac{G_F m_\mu^5}{192\pi^3}. \tag{43}$$

Assuming the standard model, G_F is determined to 1 part in 10^5 from muon lifetime measurements. If there are exotic contributions to the muon lifetime, the measured value of G_F would be shifted from the true value. Since

$$m_W \propto G_F^{-1/2}, \tag{44}$$

the 0.1% uncertainty on m_W corresponds to a 0.4% shift in the muon lifetime. Finally, the CKM matrix element V_{ud} is determined from the rate of nuclear β-decays relative to the muon lifetime. The assumption of unitarity on the CKM matrix gives us the following constraint on the first row:

$$|V_{ud}|^2 + |V_{us}|^2 + |V_{ud}|^2 = 1. \tag{45}$$

The experimental determination is [37]:

$$|V_{ud}|^2 + |V_{us}|^2 + |V_{ud}|^2 = 0.991 \pm 0.005. \tag{46}$$

The uncertainty on this constraint corresponds to a 0.5% shift in the muon lifetime. Additional contributions to the muon decay rate would lead to a downward shift in the determined value of $|V_{ud}|^2$ from the true value. We conclude that exotic decay modes of the muon with branching ratios totaling 0.5% are possible without contradicting current measurements or tests of the standard model.

As a concrete example of such an exotic process we consider R-parity-violating supersymmetric models. These models lead to lepton-number-violating vertices with couplings λ, and muon decay processes such as $\mu \to e\bar{\nu_\tau}\nu_\tau$ as shown in Fig. 1. The matrix element for these decays turns out to have the same form as for the standard W-exchange. The current constraints on the couplings λ are reviewed in Ref. [38]. These constraints allow a branching ratio of 0.4% for the process in Fig. 5.

Similar processes are allowed for anomalous lepton production as shown for example in Fig. 5. Estimates for allowed rates are in progress [39]. These diagrams involve the λ' couplings. Currently, the best limit on one of these couplings, λ'_{231}, is from ν_μ deep-inelastic scattering, so existing neutrino data is already providing constraints! The search for these types of effects at the muon storage ring could be input into a decision on whether to build a muon-proton collider where they could be studied in more detail.

As a start on estimating the capabilities of an experiment at the neutrino source, we consider the detector concept illustrated in Fig. 6. This concept consists of a repeating sequence of 1.5 mm-thick Tungsten sheets with Silicon tracking, separated by 4 mm. Tungsten, being dense, provides a high target mass while being thin enough for a produced τ to have a high probability of hitting the Silicon. The impact parameter of the τ decay products is typically 90 microns with a broad distribution, so we would like a hit resolution of 5 microns or better. Although there is a lot of multiple scattering in the tungsten, the short extrapolation distance provides for a good impact parameter resolution on the τ decay products. This configuration has been optimized for a 50 GeV muon beam. For lower energy beams, the planes should be spaced more closely, and the Tungsten thickness perhaps reduced. Studies of detectors with passive target mass and tracking with emulsion sheets [40] suggest that we can expect τ reconstruction efficiencies as high as 30%.

We would propose placing such a detector in a magnetic field, and measuring the momentum of muons and hadrons should be straightforward. However, each Tungsten sheet is 0.4 radiations lengths thick, and while we should obtain good energy resolution for electromagnetic showers, determining the electron charge will be difficult. We estimate it would take roughly a 4 Tesla field transverse to the beam direction to have a good chance of measuring the charge of a 50 GeV electron. Even then, detailed studies are needed to determine if this can be done reliably.

A total mass of 6 tons of Tungsten corresponds to 200 m^2 of Silicon tracking. For 5×10^{20} muon decays at 50 GeV, we expect a total of 35 billion neutrino interactions. Obviously there is much potential for sensitivity to very rare exotic processes, but detailed simulations and studies of possible Silicon tracking technologies are needed to quantify this.

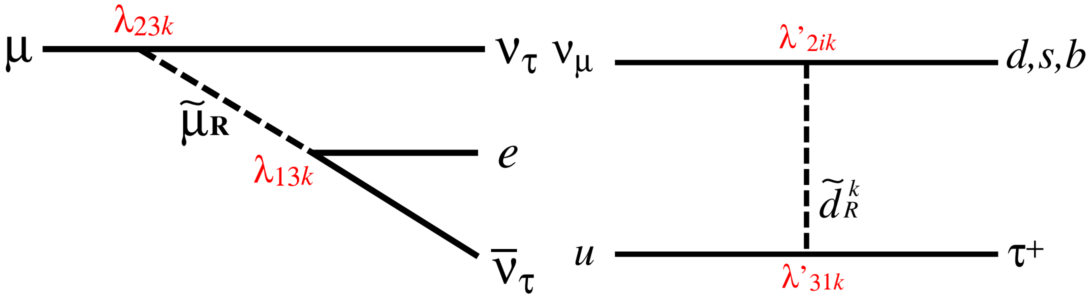

FIG. 5. Example of exotic muon decay in R-parity-violating SUSY (Left), and an example of an exotic neutrino interaction in R-parity-violating SUSY (Right).

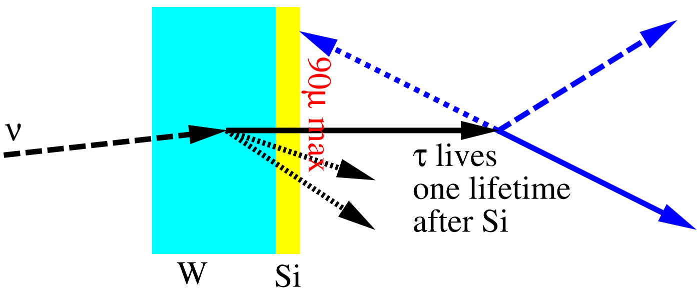

FIG. 6. One plane of a detector for τ production.

REFERENCES

[1] S. Adler, Phys.Rev.143, (1966), 1144-1155.
[2] C. Boros et al., hep-ph/9810220, Oct. 1998.
[3] S.A. Kulagin, hep-ph/9812532, Aug. 1998.
[4] K.J. Eskola et al. hep-ph/9906484, May, 1999.
[5] C.Arroyo, B.J.King *et. al.*, Phys. Rev. Lett. **72**, 3452 (1994).
[6] K.S.McFarland *et al.*, CCFR, Eur. Phys. Jour. **C1**, 509 (1998)
[7] C.H.Llewellyn Smith, Nucl. Phys. **B228**, 205 (1983)
[8] R.Bernstein *et. al.*, NuTeV Collaboration, Fermilab-TM-1088 (1994).
[9] E.A.Paschos and L. Wolfenstein, Phys. Rev. **D7**, 91 (1973)
[10] K.S.McFarland, NuTeV collaboration, to be published in the proceedings of the XXXI-IIrd Rencontres de Moriond (1998); J. Yu, NuTeV collaboration, to be published in the proceedings of the DIS98, Brussel, Belgium, Fermilab-Conf-98/200-E (1998)
[11] H. Schellman, to be published in the proceedings of the Workshop on Physics at the First Muon Collider, Fermilab, Batavia, IL, USA, Nov. 1997.
[12] D.A.Harris & K.S.McFarland, MIT-LNS-98-276, to be published in the proceedings of the Workshop on Physics at the First Muon Collider, Fermilab, Batavia, IL, USA, Nov. 1997
[13] B.J.King, to be published in the proceedings of the Workshop on Physics at the First Muon Collider, Fermilab, Batavia, IL, USA, Nov. 1997.
[14] U.K Yang and A. Bodek, *UR-1543*, Submitted to Phys. Rev. Lett, hep-ex/9809480 (1998)
[15] U. Baur and M. Demarteau, "Precision Electroweak Physics at Future Collider Experiments," Fermilab-Conf-96/423 (1996).
[16] P. Villain *et al.*, Phys. Lett. **B335**:246 (1994). See also Phys. Lett. **B302**:351 (1993) and Phys. Lett. **B281**:159 (1992).
[17] D. Yu. Bardin and V. A. Dokuchaeva, JINR E2-86-260 (1986).
[18] U. Baur, "Electroweak Radiative Corrections to W Boson Production at the Tevatron", SUNY-Buffalo preprint UB-HET-98-02, Sep 1998 (e-Print Archive: hep-ph/9809327).
[19] E. Sather, Phys. Lett. **B274** (1992) 433.
[20] M.Gronau, C.N. Leung, and J.L. Rosner, Phys. Rev. **D29**, 2539 (1984).
[21] R. E. Shrock, Phys. Rev. **D24**, 1232 (1981).
[22] T. Bolton, L. Johnson, and D. McKay, Phys. Rev. D **56** (1997) 2970.
[23] A. Vaitaitis *et al.*, Phys. Rev. Lett. **83** (1999) 4943.
[24] J. Formaggio *et al.*, Phys. Rev. Lett. **XXX** (2000) XXX.
[25] *Review of Particle Physics* Eur. Phys. J. C. 3,320 (1998).
[26] R. Shrock, Phys. Rev. D **24** (1981) 1232.
[27] B.W.Lee and R.E.Shrock, Phys. Rev. **D16** 1444 (1977).
[28] M.Frank, Phys. Rev. D60:093005 (1999).
[29] G.C.McLaughlin and J.N.Ng, hep-ph/9909558.
[30] J.F.Beacom and P.Vogel, Phys. Rev. Lett. **83**, 5222 (1999).
[31] A.V.Derbin, Phys. of Atomic Nuclei, **57**, 222 (1994) [Yad. Fiz. **57**, 236 (1994)], and A.I.Derbin *et al.,* JETP Lett. **57**, 768 (1993).

[32] D.A.Krakauer *et al.*, Phys. Lett. **B252**, 177 (1990); R.C.Allen *et al.*, Phys. Rev. **D47**, 11 (1993).
[33] MFukugita and S.Yazaki, Phys. Rev. **D36** (1987) 3817.
[34] R.Barbieri and R.N.Mohapatra, Phys. Rev. Lett. **61** (1988) 27, and J.M. Lattimer and J.Cooperstein, Phys. Rev. Lett. **61** (1988) 23.
[35] Private discussions with Norbert Holtkamp, Fermilab.
[36] See Steve Geer's talk at the 2-day meeting. Number of events (5000) was quoted for a 50 kTon detector at L=2800 km and a 20 GeV muon storage ring.
[37] Review of Particle Properties, C. Caso *et. al.*, Euro. Phys. J. **C**3, 1 (1998).
[38] H. Dreiner, hep-ph/9707435
[39] Chris Quigg, private communication
[40] K. Kodama *et. al.* (OPERA Collaboration), CERN/SPSC 98-25.
A. E. Asratyan *et. al.*, hep-ex/0002019